Numerical Acoustic Models Including Viscous and Thermal losses: Review of Existing and New Methods

P. Risby Andersen[1], V. Cutanda Henríquez[2], N. Aage[3]
Technical University of Denmark, Ørsteds Plads, Building 352,DK-2800, Kgs. Lyngby , Denmark.
[1]*prand@elektro.dtu.dk* [2]*vcuhe@elektro.dtu.dk* [3]*naage@mek.dtu.dk*

S. Marburg[4]
Technical University of Munich, Boltzmannstr. 15, 85748 Garching b. München, Germany.
[4]*steffen.marburg@tum.de*

Introduction

This work presents an updated overview of numerical methods including acoustic viscous and thermal losses. Numerical modelling of viscothermal losses has gradually become more important due to the general trend of making acoustic devices smaller. Not including viscothermal acoustic losses in such numerical computations will therefore lead to inaccurate or even wrong results. Both, Finite Element Method (FEM) and Boundary Element Method (BEM), formulations are available that incorporate these loss mechanisms. Including viscothermal losses in FEM computations can be computationally very demanding, due to the meshing of very thin boundary layers and the added degrees of freedom[3]. These implications can be avoided using the BEM with losses,[**?**] but other shortcomings affect this formulation as well. Through a simple academic test case, well established acoustic implementations and a newly proposed coupled FEM and BEM method including viscothermal dissipation are compared and investigated.

Dissipative Finite Element models

For general geometries mainly two FEM approaches exist, with the most common being the full linearised Navier-Stokes (FLNS). This approach has been studied by several authors[1][2][3][4]. Assuming no simplification the linearised Navier-stokes, continuity and energy equations are solved using classical FEM

$$i\omega\rho_0\mathbf{u} = \nabla\cdot\left(-p\mathbf{I}+\mu\boldsymbol{\sigma}-\left(\frac{2}{3}\mu-\mu_B\right)(\nabla\cdot\mathbf{u})\,\mathbf{I}\right) \quad (1)$$

$$i\omega\rho+\rho_0\nabla\cdot\mathbf{u} \quad (2)$$

$$i\omega\rho 0 C_p T = -\nabla\cdot(-\lambda\nabla T)+i\omega\alpha_0 T_0 p \quad (3)$$

$$\rho=\rho_0\left(\beta_T p-\alpha_0 T\right) \quad (4)$$

Usually the resulting system of equations is expressed from the acoustic pressure p, particle velocity $\mathbf{u}$ and temperature T. The remaining quantities are; the static density ρ_0, the static temperature T_0, the dynamic viscosity μ, the bulk viscosity μ_B, the heat capacity at constant pressure C_p, the thermal conductivity λ, the coefficient of thermal expansion α_0 and the isothermal compressibility β_T. Further $\boldsymbol{\sigma}=\nabla\mathbf{u}+\nabla\mathbf{u}^T$.

Another interesting FEM approach proposed by Kampinga is the sequential linearized Navier-Stokes (SLNS). By an orders of magnitude analysis, Kampinga showed that it is possible to decouple the fundamental equations into three independent equations by neglecting less important terms[5]. In the presented simulations only the FLNS implementation will be used for comparison. More specifically the FLNS implementation found in COMSOL Multiphysics.

Dissipative Boundary Element model

Several authors have shown the possibility of BEM models including losses. Dokumaci[6][7] and Karra[8] presented different approaches where viscothermal losses were included int the BEM. But both include some restrictions using approximations or neglecting viscosity. Later, Cutanda extended the concept of Karra to include both viscous and thermal losses, without any simplification[9][10][11][12]. The BEM presented by Cutanda takes its starting point at the Kirchoff decomposition of the Navier-Stokes equations,

$$\nabla^2 p_a + k_a^2 p_a = 0 \quad (5)$$

$$\nabla^2 p_h + k_h^2 p_h = 0 \quad (6)$$

$$\nabla^2 \vec{v}_v + k_v^2 \vec{v}_v = 0 \quad \text{with} \quad \nabla\cdot\vec{v}_v = 0 \quad (7)$$

where p_a, p_h,$\vec{v}_v$,k_a,k_h and k_v are the acoustic pressure, thermal pressure, viscous velocity, acoustic wavenumber, thermal wavenumber and viscous wavenumber, respectively. The equation-set reassembles three Helmholtz equations, all discretized, using collocation and coupled through the boundary, assuming isothermal and non-slip boundary conditions. While the method has shown the capability to tackle large complex problems [13] some shortcomings are still present. In general coupling of the equations is handled through first and second tangential derivatives of the acoustic pressure using a simple finite difference scheme, presumably having an impact on the general accuracy. The implementation used in the further comparison is the open source OpenBEM MATLAB library[15], for axi-symmetric and 3D cases with losses, extended by the first author to include losses in 2D.

New coupled Finite Element and Boundary Element Method with dissipation

The starting point of the coupled FEM and BEM is the Kirchhoff decomposition, discretizing Equation (5) using FEM and Equation (6) and (7) with BEM. The presented derivation is very compact and we refer the reader to a more thorough derivation of the pure BEM in [10]. The discretized equations yields

$$\left(-\mathbf{K}_a - k_a^2\mathbf{M}_a\right)\mathbf{p}_a + \boldsymbol{\Theta}_a\frac{\partial \mathbf{p}_a}{\partial n} = 0 \tag{8}$$

$$\mathbf{A}_h\mathbf{p}_h - \mathbf{B}_h\frac{\partial \mathbf{p}_h}{\partial n} = 0 \tag{9}$$

$$\mathbf{A}_v\mathbf{v}_{v,x} - \mathbf{B}_v\frac{\partial \mathbf{v}_{v,x}}{\partial n} = 0 \tag{10}$$

$$\mathbf{A}_v\mathbf{v}_{v,y} - \mathbf{B}_v\frac{\partial \mathbf{v}_{v,y}}{\partial n} = 0 \tag{11}$$

Where $\mathbf{K}_a$, $\mathbf{M}_a$, $\boldsymbol{\Theta}_a$ are the acoustic finite element stiffness, mass and boundary mass matrix, respectively. $\mathbf{A}$ is the double layer potential and $\mathbf{B}$ the single layer potential. The subscripts a, h or v specifies either acoustic, thermal or viscous modes. Further, Equation (7) is split into its Cartesian components. The discretized equations will be coupled through the boundary conditions expressed in local normal and tangential form as

$$T = \tau_a p_a + \tau_h p_h = 0 \tag{12}$$

$$v_{b,n} = \phi_a\frac{\partial p_a}{\partial n} + \phi_h\frac{\partial p_h}{\partial n} + v_{v,n} \tag{13}$$

$$v_{b,t} = \phi_a\frac{\partial p_a}{\partial t} + \phi_h\frac{\partial p_h}{\partial t} + v_{v,t} \tag{14}$$

With T being the temperature, τ_a and τ_h are frequency dependent complex constant relating p_a and p_h to the temperature. Similar ϕ_a and ϕ_h are frequency dependent complex constants defined from fluid viscosity. The boundary velocity can be specified from the normal and tangential velocities $v_{b,n}$ and $v_{b,t}$, respectively. It is important to note that $\partial/\partial t$ is the tangential derivative and not related to time. To account for the change in basis, a coordinate transformation between local and Cartesian coordinates are necessary, given by

$$v_{v,x} = n_x v_{v,n} + t_x v_{v,t} \tag{15}$$

$$v_{v,y} = n_y v_{v,n} + t_y v_{v,t} \tag{16}$$

The general idea is to couple the discretized equations through the boundary conditions. Since the viscous velocity is considered rotational, $\nabla \cdot \vec{v}_v = 0$, it must obey the following in local coordinates

$$\frac{\partial \mathbf{v}_{v,n}}{\partial n} + \frac{\partial \mathbf{v}_{v,t}}{\partial t} = 0 \tag{17}$$

It is further possible to relate the normal viscous velocity to the Cartesian description through

$$\mathbf{v}_{v,n} = \mathbf{n}_x \circ \mathbf{v}_{v,x} + \mathbf{n}_y \circ \mathbf{v}_{v,y} \tag{18}$$

Where $\circ$ is the so-called Hardamard product, or element-wise product. Taking the normal derivative of Equation (18) and using Equation (10), (11), (15) and (16) it is obtained that

$$\begin{aligned}\frac{\partial \mathbf{v}_{v,n}}{\partial n} = &\left(\mathbf{N}_1 \circ \left(\mathbf{B}_v^{-1}\mathbf{A}_v\right)\right)\mathbf{v}_{v,n} \\ &+ \left(\mathbf{N}_2 \circ \left(\mathbf{B}_v^{-1}\mathbf{A}_v\right)\right)\mathbf{v}_{v,t}\end{aligned} \tag{19}$$

where,

$$\mathbf{N}_1 = \mathbf{n}_x\mathbf{n}_x^T + \mathbf{n}_y\mathbf{n}_y^T \tag{20}$$

$$\mathbf{N}_2 = \mathbf{n}_x\mathbf{t}_x^T + \mathbf{n}_y\mathbf{t}_y^T \tag{21}$$

Now the second term in Equation (17) can be found by taking the tangential derivative of Equation (14), yielding

$$\frac{\partial \mathbf{v}_{v,t}}{\partial t} = \frac{\partial \mathbf{v}_{b,t}}{\partial t} - \phi_a\Delta_t\mathbf{p}_a - \phi_h\Delta_t\mathbf{p}_h \tag{22}$$

Combining Equation (17), (19) and (22) results in

$$\begin{aligned}&\frac{\partial \mathbf{v}_{b,t}}{\partial t} - \phi_a\Delta_t\mathbf{p}_a - \phi_h\Delta_t\mathbf{p}_h \\ &\quad + \left(\mathbf{N}_1 \circ \left(\mathbf{B}_v^{-1}\mathbf{A}_v\right)\right)\mathbf{v}_{v,n} \\ &+ \left(\mathbf{N}_2 \circ \left(\mathbf{B}_v^{-1}\mathbf{A}_v\right)\right)\mathbf{v}_{v,t} = 0\end{aligned} \tag{23}$$

The above is later used to assemble the final system of equations. Coupling of FEM and BEM is achieved through the tangential and normal derivatives. By taking the normal derivative of the isothermal boundary condition, Equation (12), and utilizing the normal derivative of Equation (13), an expression for the normal acoustic pressure derivative can be established

$$\frac{\partial \mathbf{p}_a}{\partial n} = -\frac{\tau_h}{\tau_a}\frac{\partial \mathbf{p}_h}{\partial n} = \left(\phi_a - \phi_h\frac{\tau_a}{\tau_h}\right)^{-1}\left(\mathbf{v}_{b,n} - \mathbf{v}_{v,n}\right) \tag{24}$$

The above is used to rewrite Equation (8) and (9), into the form

$$\begin{aligned}&\left(-\mathbf{K}_a + k_a^2\mathbf{M}_a\right)\mathbf{p}_a \\ &= -\boldsymbol{\Theta}_a\left(\phi_a - \phi_h\frac{\tau_a}{\tau_h}\right)^{-1}\left(\mathbf{v}_{b,n} - \mathbf{v}_{v,n}\right)\end{aligned} \tag{25}$$

$$\mathbf{A}_h\mathbf{p}_h + \mathbf{B}_h\frac{\tau_a}{\tau_h}\left(\phi_a - \phi_h\frac{\tau_a}{\tau_h}\right)^{-1}\left(\mathbf{v}_{b,n} - \mathbf{v}_{v,n}\right) = 0 \tag{26}$$

Using Equation (17), (23), (25) and (26), a complete system of equations can be established, with the system matrix $\mathbf{H}$ given by

$$\mathbf{H} = \begin{bmatrix} \mathbf{H}_{11} & \mathbf{0} & \mathbf{H}_{13} & \mathbf{0} \\ \mathbf{0} & \mathbf{A}_h & \mathbf{H}_{23} & \mathbf{0} \\ \phi_a\nabla_t & \phi_h\nabla_t & \mathbf{0} & \mathbf{I} \\ -\phi_a\Delta_t & -\phi_h\Delta_t & \mathbf{H}_{43} & \mathbf{H}_{44} \end{bmatrix} \tag{27}$$

and the matrix entries defined as

$$\mathbf{H}_{11} = -\mathbf{K}_a - k_a^2 \mathbf{M}_a \tag{28}$$

$$\mathbf{H}_{13} = -\mathbf{\Theta}_a \left(\phi_a - \phi_h \frac{\tau_a}{\tau_h} \right)^{-1} \tag{29}$$

$$\mathbf{H}_{23} = -\mathbf{B}_h \frac{\tau_a}{\tau_h} \left(\phi_a - \phi_h \frac{\tau_a}{\tau_h} \right)^{-1} \tag{30}$$

$$\mathbf{H}_{43} = \mathbf{N}_1 \circ \left(\mathbf{B}_v^{-1} \mathbf{A}_v \right) \tag{31}$$

$$\mathbf{H}_{44} = \mathbf{N}_2 \circ \left(\mathbf{B}_v^{-1} \mathbf{A}_v \right) \tag{32}$$

The right-hand side vector becomes

$$\mathbf{f} = \begin{bmatrix} -\left(\phi_a - \phi_h \frac{\tau_a}{\tau_h} \right)^{-1} \mathbf{\Theta}_a \mathbf{v}_{b,n} \\ -\frac{\tau_a}{\tau_h} \left(\phi_a - \phi_h \right)^{-1} \mathbf{B}_h \mathbf{v}_{b,n} \\ \mathbf{v}_{b,t} \\ -\nabla_t \mathbf{v}_{b,t} \end{bmatrix} \tag{33}$$

and the resulting complete coupled FEM and BEM system is

$$\mathbf{H} \begin{bmatrix} \mathbf{p}_a \\ \mathbf{p}_h \\ \mathbf{v}_{v,n} \\ \mathbf{v}_{v,t} \end{bmatrix} = \mathbf{f} \tag{34}$$

Making it possible to solve for the domain acoustic pressure $\mathbf{p}_a$ and the boundary variables $\mathbf{p}_h$,$\mathbf{v}_{v,n}$ and $\mathbf{v}_{v,t}$. It should be noted that the coupled FEM and BEM formulation inherits the same tangential derivative finite difference scheme as in the pure BEM.

Test case

The new coupled FEM-BEM approach is in the following compared against the regular FEM and BEM implementations with losses. To evaluate the methods a simple two dimensional study case of a viscometer like geometry were performed. Similar to the Greenspan viscometer found in [14]. A description of dimensions and boundary conditions are seen in Figure 1. All methods are compared against a reference FEM simulation with 7 million degrees of freedom.

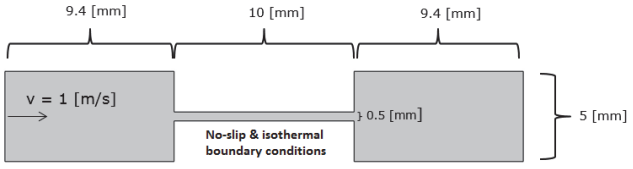

Figure 1: Two dimensional viscometer geometry with dimensions and boundary conditions. The boundary conditions are an boundary velocity of 1 [m/s] on the left boundary and all boundaries being isothermal and following the no-slip conditions.

One of the main ideas behind the coupling of FEM and BEM for modeling of viscous and thermal losses is to avoid meshing of boundary layers, but still utilizing a domain method, making evaluation of field points unnecessary. This statement is tested with two types of simulations. Firstly, a study of the error over frequency for the coarsest mesh of Figure 2 was performed. Simulation results are seen in Figure 3, comparing FEM with the FEM-BEM coupled formulation. Both FEM simulations for the coarse mesh and a similar mesh utilizing a frequency dependent one element boundary layer are shown. The FEM-BEM implementation shows a reduced error over a broad range of frequencies as compared to FEM, using significantly fever degrees of freedom. But near 2kHz, the resonance of the viscometer, the errors of the two methods are more comparable. Especially, the FEM with a single element boundary layer mesh seems to show a more stable error behavior around the resonance. The FEM-BEM implementation has an increase in error for low frequencies.

Secondly, a series of convergence studies were performed for seven gradually increasing mesh densities, shown in Figure 2. Convergence of a large amount of frequencies were carried out. Figure 4 show four studies below the resonance frequency. In general FEM shows well convergence behavior. On the other hand, both BEM and FEM-BEM have more complicated convergence behavior. Especially, as frequency decreases and mesh density increases. A proposed explanation is the use of finite difference as coupling method. Since, as frequency decreases the pressure in the domain becomes more and more uniform. With increasing mesh density the nodal pressure values will become near equal, resulting in near zero values, when using finite difference to evaluate the pressure derivatives. It should be noted that for higher frequencies and near resonance the BEM shows very good convergence, having a significant lower error for a similar amount of degrees of freedom compared to FEM. Nonetheless, it has been necessary to leave out these results.

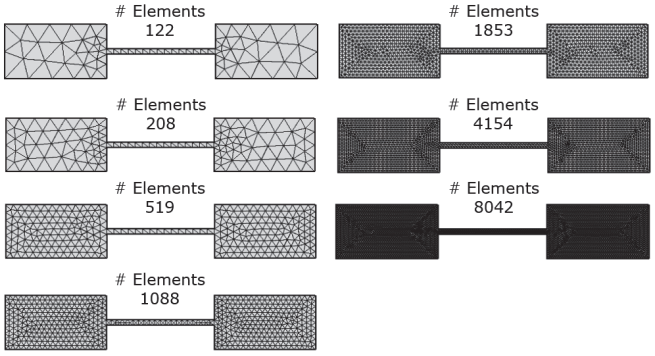

Figure 2: Different meshes used to evaluate the performance of the different numerical implementations. All elements are second order Lagrange elements.

Conclusion

A comparison of the existing full numerical implementations with losses was presented. Further a new coupled FEM and BEM formulation was derived and implemented, showing an extended reduction of error over a broad range of frequencies compared to the FEM. Unfortunately, convergence studies show only poor or no convergence. Especially, low frequencies are problematic, presumably due to the use of finite difference as coupling method.

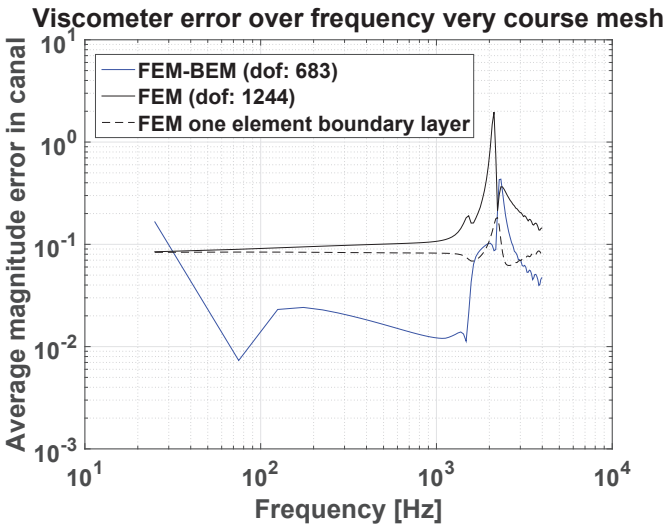

Figure 3: Average relative magnitude error in the canal using the coarsest mesh in Figure 2. The blue line is the error for the new coupled FEM and BEM approach, the black line is the error with FEM and the dashed black line is the error for FEM but with an added frequency depended single element boundary layer mesh.

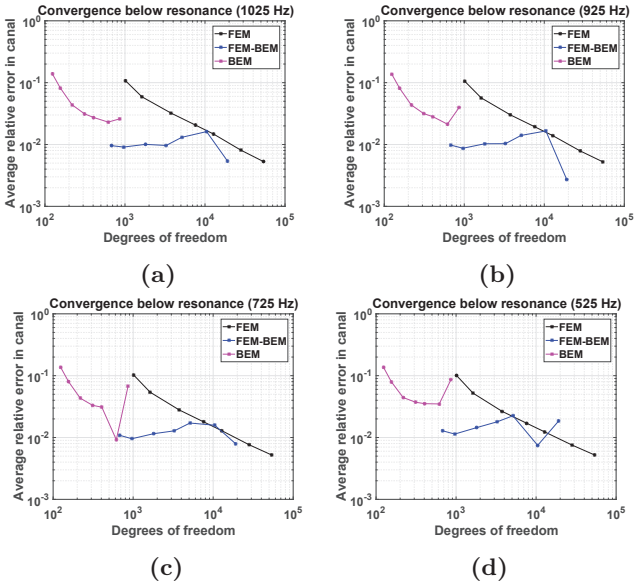

Figure 4: Convergence at different frequencies below the resonance frequency of the viscometer. (a) 1025 Hz (b) 925 Hz (c) 725 Hz (d) 525. Meshes used are those of Figure 2.

References

[1] Malinen M., Lyly M., Raback P., Karkkainen A. and Karkkainen L.: A finite element method for the modeling of thermo-viscous effects in acoustics. European Congress on Computational Methods in Applied Science and Engineering, 24-28 July (2004), jyväskylä (Finland)

[2] Nijhof M.J.J, Wijnant Y.H. and de Boer A.: An acoustic finite element including viscothermal effects. International Congress on Sound and Vibration, 9-12 July (2007), Cairns (Australia)

[3] Joly N.: Finite element modeling of thermoviscous acoustics in closed cavities, Euronoise , 29 June- 4 July (2008), Paris (France)

[4] Kampinga W. R., Wijnant Y. H. and de Boer A.: Performance of Several Viscothermal Acoustic Finite Elements, Acta Acust. Acust., **96** (2010), 115-124

[5] Kampinga R.: Viscothermal acoustics using finite elements analysis tools for engineers, Ph.D thesis, University of Twente, Enschede (2010)

[6] Dokumaci E.: An integral equation formulation for boundary element analysis of acoustic radiation problems in viscous fluids. Journal of Sound and Vibration **147** (1991), 335-348

[7] Dokumaci E.: Prediction of the effects of entropy fluctuations on sound radiation from vibrating bodies using an integral equation approach. Journal of Sound and Vibration **186** (1995), 805-819

[8] Karra C. and Tahar M.: An integral equation formulation for boundary element analysis of propagation in viscothermal fluids. Journal of the Acoustic Society of America **102** (1997) , 1311-1318

[9] Cutanda Henríquez V.: Numerical transducer Modeling. Ph.D. thesis, Technical University of Denmark, Lyngby 2002.

[10] Cutanda Henríquez V. and Juhl P. M.: An axisymmetric boundary element formulation of sound wave propagation in fluids including viscous and thermal losses. Journal of the Acoustic Society of America **134** (2013), 3409-3418

[11] Cutanda-Henríquez V. and Juhl P. M.: Implementation of an Acoustic 3D BEM with Visco-Thermal Losses. Inter-noise, 15-18 Sept. (2013), Insbruck (Austria).

[12] Cutanda-Henríquez V. and Juhl P. M.: verification of an Acoustic 3D BEM with Visco-Thermal Losses. Inter-noise, 15-18 Sept. (2013), Insbruck (Austria).

[13] Cutanda Henríquez V., Risby Andersen P., Søndergaard Jensen J., Møller Juhl P., Sánchez-Dehesa J.: A Numerical Model of an Acoustic Metamaterial Using the Boundary Element Method Including Viscous and Thermal losses. Journal of Computational Acoustics, **25** (2017), 1750006

[14] Gillis K. A., Mehl J. B. and Moldover M. R.: Greenspan acoustic viscometer for gases. Review of Scientific Intruments, **67** (1996), 1850

[15] Cutanda Henríquez V., Juhl P.M.:, OpenBEM - An open source Boundary Element Method software in Acoustics, Internoise 2010, 13-16 Jun. 2010, Lisbon (Portugal).